Synthesis of zinc ferrite (ZnFe₂O₄) by mechanical grinding and calcination with a magnetite/maghemite precursor obtained by coprecipitation, its influence on crystalline, morphological and thermal properties, for its potential use at high temperatures.

Síntesis de ferrita de zinc (ZnFe₂O₄) mediante molienda mecánica y calcinación con un precursor de magnetita/maghemita obtenido por coprecipitación, su influencia en las propiedades cristalinas, morfológicas y térmicas, para su potencial uso a altas temperaturas.

E.M. García-Rosales¹, M. G. Rosales-Sosa²*, I. A. Facundo-Arzola², M. García-Yregoi², C. V. Reyes-Guzmán², Y.M. Rangel-Hernández², B. I. Rosales-Sosa²

¹Facultad de Ciencias Químicas, Universidad Autónoma de Coahuila, Boulevard Venustiano Carranza 935, República, Saltillo, C.P. 25280, México.

² Facultad de Metalurgia, Universidad Autónoma de Coahuila, Boulevard Pape km. 4.5, zona universitaria, C.P. 25750. Monclova Coahuila, México.

Sent date: January 21, 2025; Accepted: May 15, 2025

Abstract

Magnetite/maghemite produced by chemical coprecipitation at different temperatures was reacted with reagent-grade zinc oxide to produce zinc ferrite (ZnFe₂O₄) by mechanical grinding. After grinding, calcination was applied at 400 °C for 3 hours. The obtained samples were characterized by X-ray diffraction (XRD), scanning electron microscopy (SEM), thermogravimetric analysis (TGA), and differential scanning calorimetry (DSC). After grinding treatment, three-phase combinations were observed of the same ferrite, which had not been reported previously and which were stabilized by the application of a calcination treatment. The crystallite sizes of the zinc ferrite (ZnFe₂O₄) compound ranged from 10.602 nm to 11.602 nm. Particle agglomerations were found by SEM, while TGA analysis shows possible moisture loss, in addition to stability at high temperatures. DSC analysis shows endothermic and exothermic reactions. The best results were obtained with magnetite/maghemite stabilized at 300 °C.

Keywords: mechanical milling, zinc ferrite, coprecipitation, magnetite/maghemite, calcination.

Resumen

La magnetita/maghemita producida por coprecipitación química a diferentes temperaturas, se hizo reaccionar con óxido de zinc grado reactivo para producir ferrita de zinc (ZnFe₂O₄) mediante molienda mecánica. Luego de la molienda, se aplicó calcinación a 400 °C durante 3 horas. Las muestras obtenidas se caracterizaron por difracción de rayos X (DRX), microscopía electrónica de barrido (MEB), análisis termogravimétrico (TGA) y calorimetría diferencial de barrido (DSC). Luego del tratamiento de molienda, se observaron combinaciones trifásicas de la misma ferrita, lo cual no había sido reportado previamente y que se estabilizaron con la aplicación de un tratamiento de calcinación. Los tamaños de cristalita del compuesto de ferrita de zinc (ZnFe₂O₄) variaron de 10.602 nm a 11.602 nm. Se encontraron aglomeraciones de partículas por medio de MEB, mientras que el análisis TGA muestra una posible pérdida de humedad, además de estabilidad a altas temperaturas. DSC muestra reacciones endotérmicas y exotérmicas. Los mejores resultados se obtuvieron con magnetita/maghemita estabilizada a 300 °C.

Palabras clave: molienda mecánica, ferrita de zinc, coprecipitación, magnetita/maghemita, calcinación.

*Corresponding author. E-mail: mrosales@uadec.edu.mx; https://doi.org/10.24275/rmiq/Mat25509

ISSN:1665-2738, issn-e: 2395-8472

1 Introduction

Zinc ferrite (ZnFe₂O₄) is a magnetic ceramic material that has been studied since the 1950s. Its magnetic properties are of great research interest because of their potential multiple applications. The uses of zinc ferrite are highly varied and include microwave devices, recording media, devices used at high frequencies, biomedical devices, and permanent and temporary magnets (Baena *et al.*, 2011).

Iron oxide with the oxides of one or more other metals combine to form ferrite, not all ferrites develop spinel structure, but many do. While bulk zinc ferrites are paramagnetic at ambient temperature, nano-crystalline zinc ferrites can be ferrimagnetic at the same temperature. Its structural formula is $(ZnFe)_x[ZnFe]_{2-x}O_4$, in which the coordination sites marked by the parentheses represent Tetrahedron A, the brackets represent Octahedron B, and x represents the degree of inversion, which is defined as the fraction of the A sites occupied by Fe³⁺. One of the precursors of the zinc ferrite compound may be Fe₂O₃ (maghemite), which can be obtained by chemical coprecipitation, which, as an easily scalable process, enables the industrial use of zinc ferrite for the manufacture of iron oxide nanoparticles. Chemical coprecipitation consists of adding Fe²⁺ salt and Fe³⁺ solutions to an excess basic medium. The advantages of this method are its simplicity and low cost, while the disadvantage is the high number of uncontrolled variables and the wide distribution of particle sizes (Baena et al., 2011). Various methods are used to obtain zinc ferrite, such as the ceramic method, sol-gel synthesis, chemical coprecipitation, the hydrothermal method, and microemulsion. In recent times, alternative synthesis methods have been explored in search of a more economical, faster, and purer process, one of which alternatives is mechanical milling, which presents the above-described advantages.

Synthesis by mechanical milling is defined as the chemical reaction induced by the direct absorption of mechanical energy (James et al., 2012). Mechanical energy is produced by the combination of impact, shear, and friction forces that activate the surface and produce defects in the network, radicals on the surface, and even break bonds, causing the activation and chemical reaction of the mixed powders (Fuentes et al., 2013). The interaction of forces during milling generates local temperatures and pressures at the points where collisions occur, which are believed to reach up to 10,000 K and 17 GPa. This, in turn, promotes a local fusion phenomenon that induces the dissolution of chemical species of immiscible elements, consequently inducing the formation of alloys that cannot be synthesized by other techniques (Baláž et al., 2009). Over the last few decades, mechanical

milling has developed from an elementary method used primarily for particle size reduction in mineral processes to a potent technique for the preparation of materials with improved mechanical and physical properties, and new phases and engineering materials (El-Eskandarany *et al.*, 2021).

Koch (1983) observed that mechanical milling induces the amorphization of the material when he subjected Ni and Nb powders to high-energy grinding. Since then, research has continued, with the combination of coprecipitation and mechanical milling reported by various authors for the preparation of both ferrites and nanoferrites. Ding et al. (1999) used a combination of both methods to produce BaFe₁₂O₁₉, CoFeO₄, and NiFeO₄, while Shi et al. (1999) produced NiFe₂O₄ and Shenoy et al. (2004) manufactured ZnFe₂O₄ via similar processes. Sheikhi *et al.* (2006) produced BaFe₁₂O₁₉. All of the authors mentioned above emphasize the possibility of obtaining ferrites by combining coprecipitation and mechanical milling. Sani et al. (2007) synthesized CoFe₂O₄ using only mechanical milling and in the same year, Rao et al. (2007), compared the separate use of coprecipitation and mechanical milling to obtain various ferrites of (Ni-Zn-In-Ti), (Ni-Zn), and (Mn-Zn). Zhigang et al. (2015) synthesized nickel ferrite nanoparticles (NiFe₂O₄) achieving a solid-state reaction through milling. The technique is considered a simple and effective synthesis method for NiFe₂O₄ and other nanomaterials. Pedrosa et al. (2016) reported the use of mechanical grinding for the synthesis of the ferrite CoFe₂O₄, while Sarkar et al. (2019) prepared the Co_{0.5}Zn_{0.5}O₄ nanoferrite by applying a combination of coprecipitation and various thermal treatments in addition to mechanical milling.

Mahdikhah et al. (2019) produced the ferrite CoFe₂O₄ via mechanical milling and Cobos et al. (2020) compared various ferrite synthesis methods, including mechanical grinding, for manufacturing ZnFe₂O₄. Navipour et al. (2020) investigated the sole use of mechanical grinding to manufacture ZnFe₂O₄, while Sukmarani et al. (2020) synthesized MnFe₂O₄ and Moravvej-Farshi et al. (2020) manufactured Ni-Zn ferrites, both using the same technique. Younes et al., (2021) synthesized CuFeO₄ via mechanical milling and Tomiczek et al., (2021) produced the ferrite CoFe₂O₄. Hejazi et al. (2024) produced ZnFe₂O₄ ferrites using the separate application of coprecipitation and mechanical milling, investigating the effects of each method on crystallinity, purity, and particle size distribution. A recent study, reported by Leal et al. (2024) investigated the production of ZnO, which can be a precursor to zinc ferrite. The study sought to produce ZnO nanoparticles using ion exchange and thermal treatments, which, although at different temperatures, were also used in the present study. According to a review by Bhattu et al. (2024), zinc ferrites have a variety of production methods

and intriguing applications. Characteristics such as crystallite size, doping, and manufacturing process influence their use in biological applications, sensors, magnetic data storage, and catalysis. Garg et al. (2024) mentioned, zinc ferrite (ZnFe₂O₄) nanoparticles are considered to be non-toxic and to have better drug delivery properties than other nanoparticles. Wider uses of ZnFe₂O₄ nanoparticles for the treatment of infectious illnesses and cancer have been documented in several research. The reduction of both organic and inorganic environmental contaminants is another advantage of these nanoparticles. Additionally, their environmental and biological uses have been extensively studied. Similarly, studies of ZnO (ferrite precursor) and its nanostructures have received recent attention for potential use in environmental applications such as solar cells (Garcia et al., 2024).

The present study sought to combine mechanical milling and the chemical coprecipitation of magnetite to synthesize a ZnFe₂O₄ ferrite, aiming to ascertain the behavior of ferrite synthesis when applied with both one precursor obtained via coprecipitation and another that was reagent grade. All this is done in the interest of the various potential applications discussed in the introduction.

2 Materials and methods

The methodology reported by previous studies was used for the present study. The technique reported by Zhang *et al.* (2009) was used for the synthesis of magnetite, wherein FeCl₃·6H₂O and FeCl₂·4H₂O (2:1 ratio) were mixed in 50 mL of deionized water, while 150 ml of deionized water was placed in a ball flask and heated to 50 °C with constant stirring. 50 ml of concentrated ammonium hydroxide was then added in order to provide a basic medium for the solution. The precursors were used to obtain the highest possible purity of the desired compound.

The iron chloride mixture was added drop by drop to the basic solution and subjected to constant stirring for 30 minutes, after the elapse of which, the precipitate was washed with 2 liters of deionized water to eliminate excess chlorides and left to dry at room temperature for three days. Finally, the product obtained was washed with 1 liter deionized water and 250 ml ethanol and left to dry at room temperature. The quantity of magnetite obtained was divided into five parts and heated at 100 °C (T1), 200 °C (T2), 250 °C(T3), 300 °C(T4), and 350 °C (T5), with a residence time of 3 hours. Once heating had been completed, the samples were left to slowly cool inside the oven, to ensure greater crystallinity.

2.1 Mechanical milling and calcination

The preparation of zinc ferrite used two powders obtained from the precursor oxides ZnO (reagent grade 99.8% pure, SkySpring Nanomaterials) nanometric zinc oxide (9–20 nm) and magnetite obtained via chemical coprecipitation.

At a 1:1 ratio, the powders were mixed, placed in a 25-ml stainless steel vial, and then placed in a RETSCH mill to apply the milling process. A 2:1 ball-material ratio was used for the milling, which was conducted at a frequency of 20 cycles per second (1200 rpm) for five hours for all samples. Dry grinding was used, without any type of additive or binder. Once the milling treatment had been completed, calcination was conducted in a Witeg brand muffle (capacity of 1200 °C) on all samples at 400 °C for three hours to stabilize the metastable phases that had formed during the mechanical milling process. The smallest crystallite sample was then characterized via scanning electron microscopy (SEM), thermogravimetric analysis (TGA), and differential scanning calorimetry (DSC).

2.2 X-ray diffraction (XRD)

This technique was applied to identify the ferrite phases and determine crystallite size, using a Bruker D8 Advance X-ray diffractometer, with a scanning range of 10 to 80° on the 2θ scale and a scanning speed of 0.01° /s. For Co-K α type radiation, the conditions of operation were 40 mA and 40 kV, while the Match 1.1 diffraction software was used to achieve sample identification.

2.2.1 Crystallite size (Debye Scherrer equation)

To achieve correct measurements of the crystallite size, the results of the XRD analyses were used with the help of the Origin 2019 (b) software together with the peak analyzer (using the longest peak as a reference) and the Gauss mathematical function included in the software. Based on the data obtained, the Debye Scherrer equation (Eq.1) was used, where each variable means the following:

$$L = \frac{0.9 \times \lambda_{a1}}{\beta_{2\theta} \times \cos \theta_{\text{max}}} \tag{1}$$

- L: the crystallite size
- λ_{a1} : the wavelength of the X-ray source implemented using Co-K α ($\lambda_{a1} = 1.54056 \text{ Å}$)
- θ_{max} : the value of the angle at 2θ for reflection (311)
- β_{2θ}: the amplitude, at half the height of the peak, for this reflection

2.3 Scanning electron microscopy (SEM)

The measurement of the magnetite level after chemical coprecipitation used a JEOL 6010 Plus scanning electron microscope with a resolution of up to 4.0 nm (at 20 kV), magnification from 8X to 300,000X, acceleration voltages from 500V to 20kV, and the secondary and backscattered electron imaging mode.

The SEM technique was used to determine the morphology, structure, and particle size. A microscope with the Hitachi cold cathode technique, model SU8230, was used. The sample was fastened to the sample holder using carbon tape. The images were taken by applying a 6 kV and 5 μ A energy level at a working distance of 2.2 nm.

2.3.1 Particle size measurement using SEM image

The public domain ImageJ 1.54g software was used to measure particle size distribution. An area of the image was selected, and particle quantification and size measurements were performed using the software's measurement functions, taking 500 nm as the standard. The particles were measured according to the researchers' interpretation, taking into account their feasible delimitation.

2.4 Thermogravimetric analysis (TGA)

Thermogravimetric analysis was used to ascertain both how the samples behave at high temperatures and their thermal stability, using, for the gas, atmospheric air with a temperature range of 30°C to 800°C at a heating rate of 10°C/min. The equipment used was a DISCOVERY Series model manufactured by the TA Instruments.

2.5 Differential scanning calorimetry analysis (DSC)

The gas used for the DSC analysis was atmospheric air, while heating, cooling and heating cycles were applied in a temperature range of 30 to 500 °C, with a heating rate of 5 °C/min. The equipment used was a DISCOVERY Series model manufactured by the TA Instruments.

3 Results and discussion

3.1 Chemical coprecipitation of magnetite and crystallography

Based on previous studies (Park *et al.*, 2001; Gnanaprakash *et al.*, 2007) the following chemical equations are adapted according to the possible growth and nucleation of the ferrites in the present study. The

iron II and III salts were mixed in an aqueous medium, immediately taking on an orange-yellowish hue, and then poured drop by drop into the basic medium, which was kept at a constant temperature of 70 °C and a pH of 14 and was subject to constant stirring. The Fe^{3+}/Fe^{2+} iron salt solution changed color when added to ammonium hydroxide, along with the formation of a black precipitate, which is the characteristic color of magnetite. This precipitate (iron oxide) is sensitive to magnetic fields (magnetite phase). Ammonium hydroxide was used as a precipitating agent due to its high solubility and alkaline conditions (pH > 11), presenting due to the formation of OH $^-$ (Eq. 2):

$$NH_3 + H_2O \longrightarrow NH^+ + OH^-$$
 (2)

This base generates OH⁻ ions slowly, enabling homogeneous nucleation with the formation of iron oxo-hydroxides, thus preventing the aggregation of disordered clusters and, therefore, controlling the reaction rate. With a pH of between 8 and 14, the reaction given in Equation 3 could have occurred during this process:

$$Fe^{2+} + 2Fe^{3+} + OH^{-} \longrightarrow Fe_{3}O_{4} + 4H_{2}O$$
 (3)

Three regimes of particle generation are applied during the precipitation process: the induction period, in which solid building units are formed (still in solution); the nucleation period, in which nucleation occurs when the concentration of building units reaches the saturation level; and the growth phase, which occurs after the nucleation period and until the reacting species in the solution reach equilibrium.

Once the nucleus generated attains the critical radius (R), it remains stable and continues with its subsequent growth, while particles with a radius of less than R will dissolve in the reaction medium. It can be said that, given a certain concentration of reactants, a maximum number of nuclei will be formed if the reaction is given sufficient time for stable nuclei to form

At short reaction times, a low number of stable nuclei are generated, as the residence time of the nuclei in the mother liquor is likely to be very short, meaning that, at low reaction times, the particle yield will be low. Increasing the reaction time should have a positive effect on the yield, as more stable nanoparticles may be generated. However, this may not be true if a range of reaction times is applied, as secondary processes, such as Ostwald ripening, may dominate, causing larger particles to grow at the expense of smaller particles, which could adversely affect the reaction yield (Thanh *et al.*, 2014).

According to stoichiometry, the reaction yield is that for every 2 moles of Fe⁺³, one mole of magnetite Fe₃O₄ is produced. The theoretical amount of magnetite produced was 10.59 g, and an actual 9.4 g was obtained at the time of synthesis, giving a

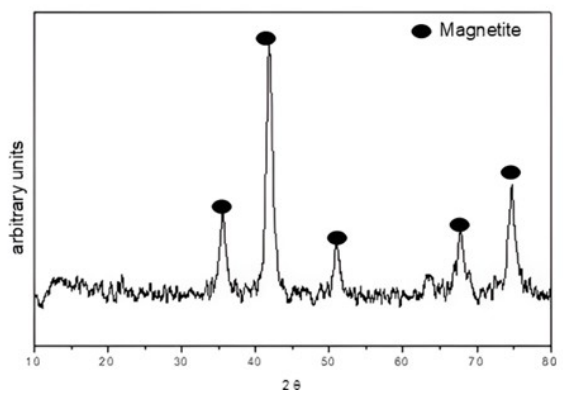


Figure 1. Diffractogram of the magnetite sample obtained via coprecipitation.

reaction yield of 88.79%. The diffractogram for the synthesis of magnetite, reveals that the highest peak corresponds to the magnetite phase (Figure 1).

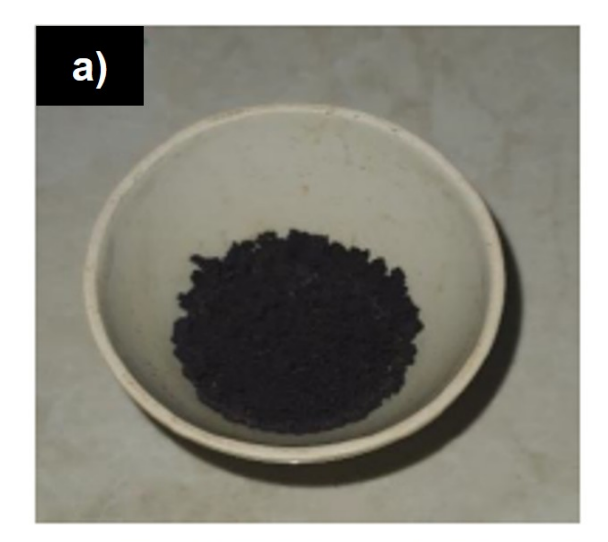
The phase obtained is consistent with the findings of Aliramajia *et al.* (2015), who synthesized magnetite by means of the sonochemical method. This phase was found at 2θ angles of 21, 35, 41, 50, 63, 67, and 75, with their corresponding reflection planes of (111), (220), (311), (400), (422), (511), (440), thus indicating that it is a magnetite compound with a cubic spinel crystalline structure. Measured with the Debye-Scherrer formula, the particle size of the magnetite phase was 9.790 nm.

3.2 Calcination of magnetite and crystallography

After thermal treatments of 100, 200, 250, 300, and 350 °C were applied to the maghemite samples, they presented a change in color from black (magnetite) to different shades of red-brown (maghemite). Further evidence of the aforementioned color change is observed in Figure 2, section a) where after synthesis by coprecipitation, a black color is obtained, and after the application of heat treatment it changes to a red-brown color (section b) (Castaño *et al.*, 1998). According to the literature (Teja *et al.*, 2009), the magnetic behavior of the iron oxide structure varies from hematite (α -Fe₂O₃), maghemite (γ -Fe₂O₃), and magnetite (Fe₃O₄) and depends on the synthesis conditions. This, therefore, confirms that the magnetite changes to the maghemite structure, as observed in the present study, occur due to the thermal treatments applied.

The diffractograms of the maghemite samples, when heated to 100, 200, 250, 300, and 350 °C, were compared to the diffraction patterns and found to be of the crystallographic phases of maghemite (Figure 3).

Table 1 shows variations ranging from 21.077-9.751 nm. A correlation is observed, in which increasing the temperature results in a reduction in particle size, behavior which could be explained by an increase in crystallinity during calcination treatment. It is un-known whether increasing the temperature further would result in a greater reduction in particle size. Contrary to what was expected, the crystallite size decreases as the temperature increases, but this is possible and already reported by Méndez and collaborators in 2019, when an increase in the calcination temperature led to a smaller crystallite size.



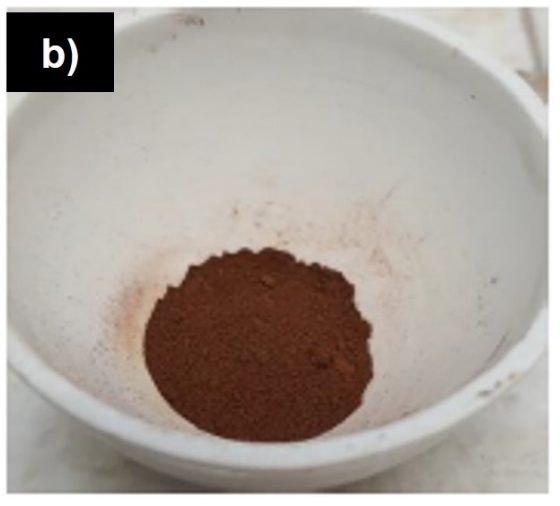


Figure 2. Change from a) magnetite to b) maghemite after calcination.

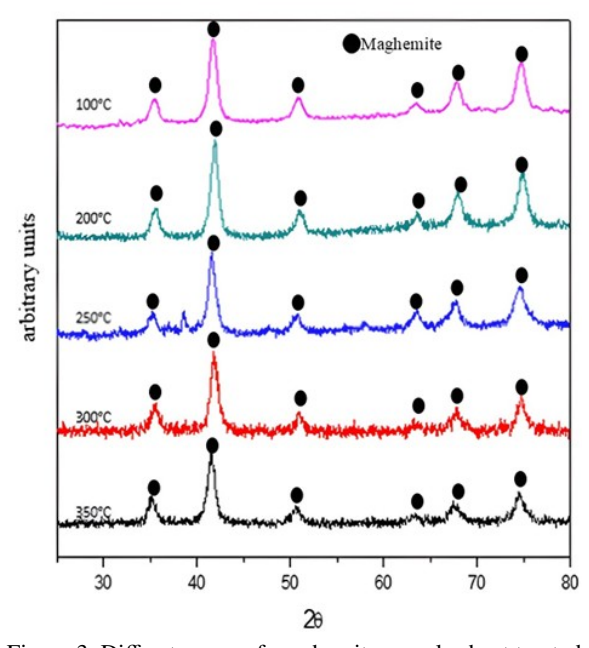


Figure 3. Diffractogram of maghemite samples heat treated at 100, 200, 250, 300, and 350 °C.

Table 1. Particle size variation of maghemite

Maghemite Sample	Heat treatment (°C)	Particle size (nm)
T1	100	21.077
T2	200	10.954
T3	250	10.7448
T4	300	10.433
T5	350	9.751

3.3 Crystallography of ferrite synthesis via mechanical milling

Figure 4 shows the diffractograms corresponding to the reactions observed after five hours of the mechanical grinding of maghemite and reagent grade zinc oxide, with the corresponding powders prepared in stoichiometric proportions, in accordance with Equation 4

$$Fe_2O_3 + ZnO \longrightarrow ZnFe_2O_4$$
 (4)

The presence of three phases is observed at the highest intensity peaks, which are very close to each other. The first peak, located at angle 41.71 in scale 2θ , indicates the presence of the franklinite phase (Zhang et al., 2008). The zincite phase is identified at angle 42 in scale 2θ (Verwey et al., 1947) while the last in this combination of phases, the maghemite phase, is identified at angle 42.5 2θ (Wyckoff, 1963). At this point, the measurement of particle size using the Debye-Scherrer equation and the Origin 2019 (b) software became difficult because a main peak could not be defined, due to the threephase combination. This triphasic combination, about which abundant information is not available in the literature, was not expected. A possible explanation is that, as the franklinite crystalline phase is just beginning to form and the zinc oxide and oxide phases still contain iron (maghemite), the phase in question cannot be identified with certainty because the phases are mixed.

From the foregoing findings, it can also be considered that, as occurs in solid systems, the equilibrium state has not been completely reached and that additional energy is required to reach the equilibrium phases as, in this case, there are mixed phase peaks. The compounds could be considered, at this point in the mixing of the phases, to be in a state of non-equilibrium and, thus, corresponding to intermediate phases. While this combination of phases may also indicate the presence of crystallinity, inclusions of different elements in a semi-defined crystalline network were observed. It would be expected that more milling time could rearrange the atoms completely to achieve a totally defined phase or structure. As the coexistence of the zincite, maghemite, and franklinite phases is observed at the most intense peaks, a thermal treatment was conducted at 400 °C, giving a residence time of three hours. The result of the thermal treatment is shown in the diffractograms presented in Figure 5. The samples were left to cool inside the oven to achieve greater crystallinity. The temperature applied, 400 °C, was able to generate sufficient activation energy to transform the maghemite and zinc oxide into the crystalline ZnFe2O4 structure, and to obtain a completely defined crystalline structure, as some had already been transformed during the mechanical grinding process. The atoms are able to migrate to the equilibrium

positions corresponding to the zinc-ferrite phase. The crystal structure corresponds to space group number Fd3m (Oh7), indicating that they present the spinel phase crystal structure. The lattice parameters observed were $a = 8.4411\text{\AA}$ (Tehranian *et al.*, 2019).

In contrast to other authors, who used a combination of coprecipitation and mechanical milling (Ding *et al.*, 2000; Shi *et al.*, 1999; Shenoy *et al.*, 2004) the present study did not use a combination of two types of precursors, namely one obtained via coprecipitation and one reactive grade. The type of synthesis applied could give rise to different results, such as the interphases reported previously.

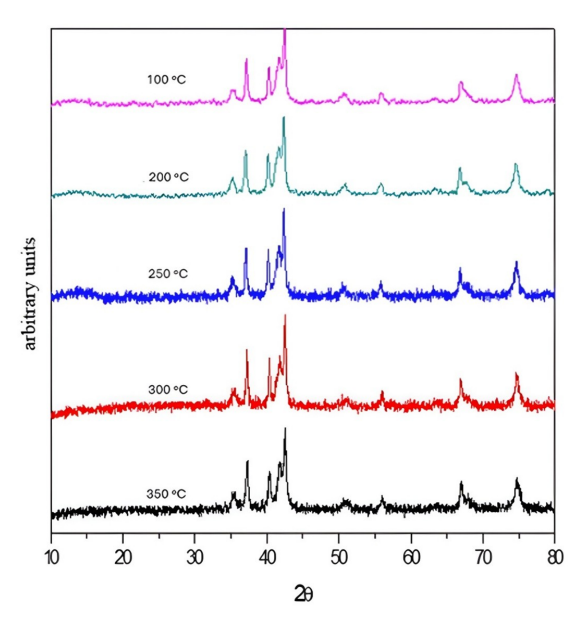


Figure 4. Diffractogram obtained for the maghemite Fe_2O_3 samples (obtained from magnetite at 100, 200, 250, 300, and 350 °C) with ZnO reacted by mechanical grinding for five hours.

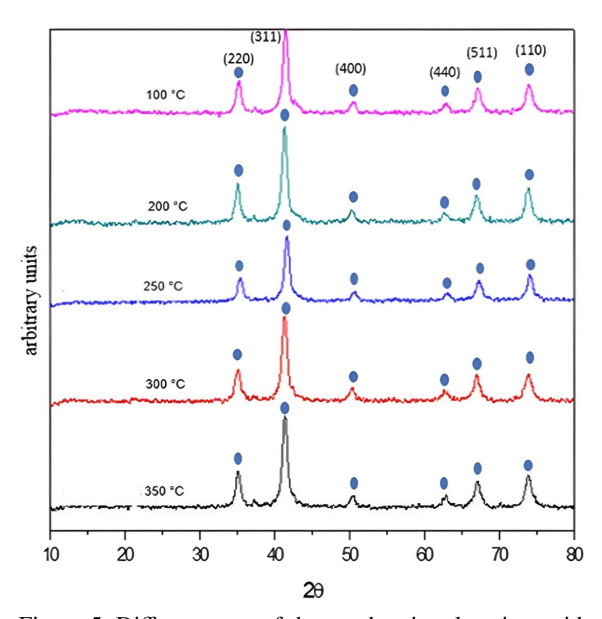


Figure 5. Diffractogram of the maghemite plus zinc oxide samples, subjected to mechanical grinding for five hours and a heat treatment at 400°C for three hours.

Table 2. Particle size variation.					
Maghemite (Fe ₂ O ₃)	Time, in hours, of	Heat treatment of	Particle size (nm)		
obtained at:	maghemite grinding	maghemite (Fe ₂ O ₃) at			
	treatment (Fe ₂ O ₃)	400 °C + ZnO grinding			
	+ ZnO.	mixture			
No treatment	No treatment	No treatment	9.790		
100 °C	5	3	11.602		
200 °C	5	3	11.421		
250 °C	5	3	11.544		
300°C	5	3	10.602		
350°C	5	3	11.473		

Those other authors who have synthesized the ZnFe₂O₄ ferrite via milling only (Shenoy *et al.*, 2004; Cobos *et al.*, 2020; Navidpour *et al.*, 2020) also did not report metaphase formation, which could be attributable to the precursors, but also confirmed that calcination treatments can be effective for the stabilization of the phases described here. Table 2 shows that the particle size of the ferrite ranges from 10.602 nm to 11.602 nm, while the maghemite particle obtained at 300 °C was found to be the smallest. However, no considerable variation in particle sizes was observed among all the samples synthesized.

The present study found that mechanical milling had a great influence on the formation of zinc ferrite after the mixtures had been milled for five hours. The mechano-chemical activation occurring during the grinding stage provided sufficient mechanical energy to initiate the solid-state reaction, which can accumulate during the plastic deformation of the crystals and the generation of their surfaces, thus producing regions of special chemical reactivity that facilitate the development of the solid phase processes. According to Takacs (1998), under the system and activation conditions of interest, solid phase reaction can occur during mechanical treatment at room temperature. However, as the grinding times applied during the present study were insufficient to complete the reaction, a heat treatment must be applied at relatively low temperatures to complete the reaction and form the zinc ferrite.

In many reactions, depending on the nature of the precursors involved, the temperature increases and results in the decomposition of both the reactants and the products themselves, requiring long reaction times that reduce the advantages of the method, thus leading studies to resort to synthesis techniques which use a solvent. No solvent was used in the present study, which is considered an advantage because it makes the process more efficient without affecting the quality of the compound obtained.

In general, these mechanical milling processes can be said to change the structure according to the movement of the cations, which, when displaced, distorts the cubic structure of the initial oxides, giving rise to new compounds. In the present study, this dynamic gave rise, albeit partially, to an arrangement corresponding to the ZnFe₂O₄ spinel-type structure.

3.4 Morphological analysis of maghemite obtained by chemical coprecipitation and calcination

The 150,000 X micrograph of maghemite calcined at 300 °C (T4) (Figure 6) enables better observation of the spherical shape of the particles that tend to form branched agglomerations, the sizes of which range from 10.2, 13.8, and 14.6 nm. These agglomerations may occur due to the method of chemical coprecipitation applied and any potential magnetic tendency of the synthesized compounds.

3.5 Morphological analysis of zinc ferrite obtained by mechanical milling

The micrograph of sample T4 shows agglomerates with irregular zinc ferrite particle shapes, an agglomeration that may be due to the mechanical grinding and/or the magnetic nature of the material. In other regions, agglomerates with diffuse sharpness are observed (Figure 7).

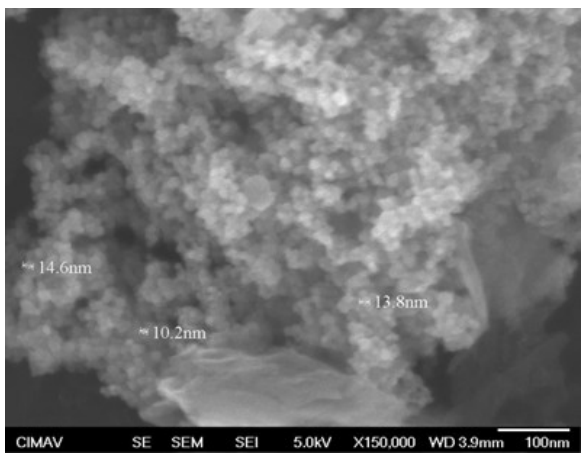


Figure 6. Morphology, at 150,000 X, of maghemite, as obtained by coprecipitation and thermal treatment at 300°C for three hours (T4).

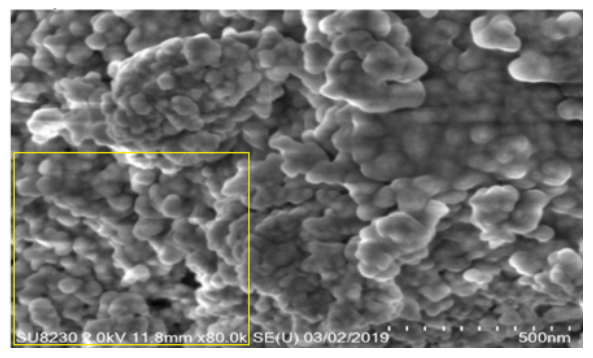


Figure 7. T4 morphological mapping (yellow rectangle area analyzed).

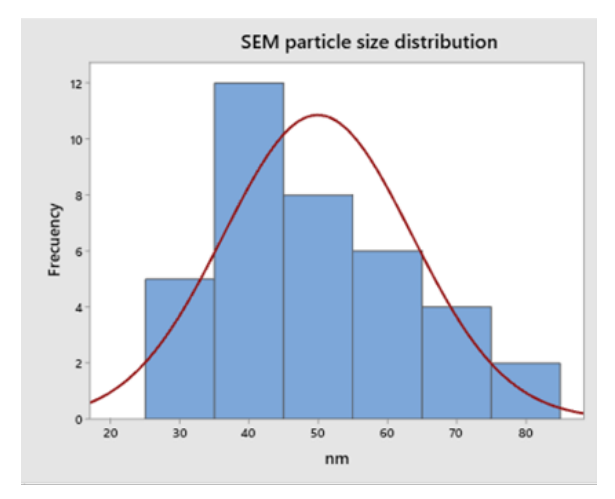


Figure 8. SEM particle size histogram.

Figure 8 shows a histogram of the particle size analyzed based on the image obtained by SEM. The yellow rectangle (Figure 7) was analyzed, and various particle sizes were found, ranging from 30 nm, 40 nm, 50 nm, 60 nm, 70 nm and 80 nm, with an average particle size of 49.93 nm, following an almost standard distribution.

Differences in particle size were found between the maghemite obtained by chemical coprecipitation and calcination and the zinc ferrite obtained by mechanical milling. This difference could be due to a greater agglomeration of particles and the methods used for their synthesis.

3.6 Thermal analyses (TGA and DSC)

As shown in Figure 9, the TGA analysis conducted on T4 shows a high level of physical and thermal stability because the material only lost 4.5% of mass, presenting small losses at 150 °C and 600 °C-700 °C. In other studies, such as that of Vidales et al. (1999), their materials lost around 20% of mass in some TGA tests under relatively similar conditions. The effects of the loss of mass could have occurred due to a certain degree of potential humidity in a precursor especially maghemite, as it had undergone coprecipitation in an aqueous solution.

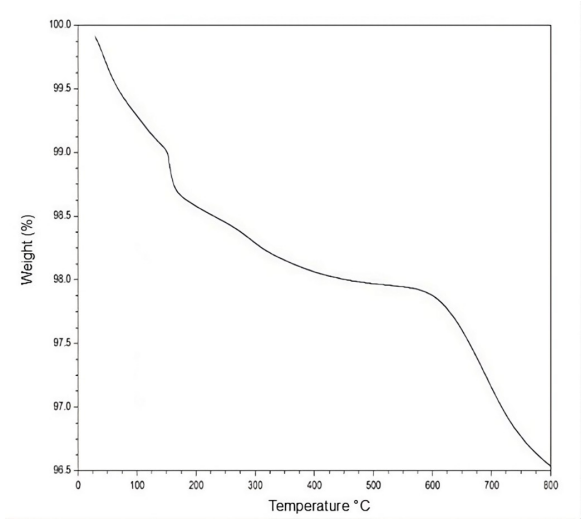


Figure 9. TGA analysis of T4.

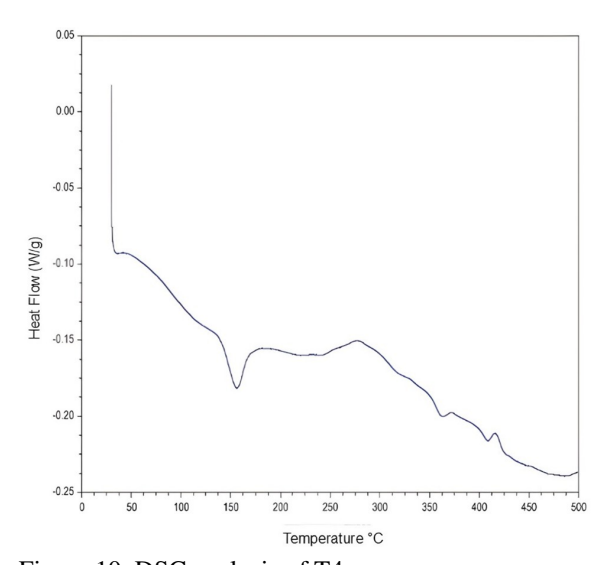


Figure 10. DSC analysis of T4.

The thermal stability observed enables the synthesized ferrites to be used in applications where they must be brought to high temperatures without losing their properties or becoming degraded. An example of the above could be its possible use in high-temperature piezoelectrics (Wang *et al.*, 2024).

Endothermic and exothermic reactions may help us understand material trends. Glass transition temperature, melting and crystallization temperatures, heat of fusion, heat of reaction, purity, heat capacity, and liquid crystal transition measurements are a few examples (Prime *et al.*,2009). The DSC conducted on the T4, shown in Figure 10, revealed three little endothermic reactions at 75°C, 150°C, and 360°C, the most significant of which being the second. Another small exothermic reaction, crystallization, is observed at 410°C, at which point, a sudden and pronounced decrease in energy is observed, wherein the heat being released proves an exothermic reaction.

When the sample undergoes exothermic processes, such as crystallization, the precursor molecules of

the zinc ferrite compound gain sufficient freedom of movement to arrange themselves into a crystalline form. All these changes could be correlated with the arrangement of the final crystalline structure and the thermal stability achieved in the material, as its structure and properties may have been completely different had these energy changes not occurred (TIP, 2023).

4 Conclusions

In the present study, chemical coprecipitation proved to be a good method of preparing magnetite, which, upon calcination, is converted into maghemite, which exhibits a reduction in particle size as its temperature increases. Mechanical milling is a useful tool for the preparation of ferrites. The reactions observed between ZnO and maghemite after five hours of grinding presented different phases, with the coexistence of the zincite (ZnO), maghemite, and franklinite phases observed, which is a hitherto unreported behavior that requires further research. This triphasic effect may be explained by the failure of the grinding conditions to provide sufficient energy to complete the reaction between zinc oxide and iron oxide, achieving only partial reactions, thus explaining the three phases observed.

The mechanochemical activation occurring during the milling stage provided sufficient mechanical energy to initiate the solid-state reaction, which can accumulate during the plastic deformation of the crystals and the generation of their surfaces, thus producing regions of special chemical reactivity that facilitate the development of the solid phase processes.

The results observed for calcination at 400 °C show that this temperature was able to generate sufficient activation energy to completely transform maghemite and zinc oxide into zinc ferrite and obtain a completely defined crystalline structure, thus eliminating the three phases and leaving only the formation of the phase of interest, zinc ferrite. The crystallite size found for this phase was 10.602-11.602 nm, with sample T4 presenting the smallest crystallite size. The spinel phase crystal structure corresponds to space group number Fd3m (Oh7). The lattice parameters were observed as a=8.4411 Å, can be concluded from the findings of the present study that thermal treatments are capable of stabilizing phases.

The scanning electron microscopy analysis shows agglomeration at various levels, even allowing for the conclusion that there may be a systematization of the agglomerations. The maghemite obtained by chemical coprecipitation and calcination had particle size variations between 10.2 and 14.6 nm. Moreover, the zinc ferrite obtained by mechanical milling had particle sizes of 30–80 nm. Differences in particle

size were found that could be due to greater particle agglomeration and the methods used for their synthesis.

The thermogravimetric analysis showed physical and thermal stability due to the low level of losses of mass (4.5%), which may have occurred due to moisture loss. These characteristics could be good in high temperature applications such as piezoelectric. The differential scanning calorimetry analysis showed endothermic and exothermic reactions at different temperature points.

Acknowledgements

The present study is supported and financed by the metallurgy and materials science academic body (UACOAH-CA-95) of the Metallurgy Faculty of the AUTONOMOUS UNIVERSITY OF COAHUILA.

References

- Aliramaji, S., Zamanian, A., & Sohrabijam, Z. (2015). Characterization and synthesis of magnetite nanoparticles by innovative sonochemical method. *Procedia Materials Science*, 11, 265–269. https://doi.org/10.1016/j.mspro.2015.11.022
- Baena, J., & Marulanda, J. (2011). Análisis de procesos químicos para la síntesis de magnetita en aplicaciones biomédicas. In *Proceedings of XVIII Congreso Argentino de Bioingeniería*, Argentina.
- Baláž, P., & Dutková, E. (2009). Fine milling in applied mechanochemistry. *Minerals Engineering*, 22(7–8), 681–694. https://doi.org/10.1016/j.mineng.2009.01.014
- Bhattu, M., Acevedo, R., & Shnain, A. (2024).

 A comprehensive review on the synthesis routes, properties and potential applications of ZnFe₂O₄ ferrites. *E3S Web of Conferences*, 588, 02014. https://doi.org/10.1051/e3sconf/202458802014
- Castaño, J., & Arroyave, C. (1998). La funcionalidad de los óxidos de hierro. *Revista de Metalurgia*, 34(3), 274–280. https://doi.org/10.3989/revmetalm.1998.v34.i3.794
- Cobos, M., de la Presa, P., Llorente, I., García-Escorial, A., Hernando, A., & Jiménez, J. (2020). Effect of preparation methods on magnetic properties of stoichiometric zinc ferrite. *Journal of Alloys and Compounds*, 849, 156353. https://doi.org/10.1016/j.jallcom.2020.156353

- De Vidales, J., López, A., Vila, E., & López, F. (1999). The effect of the starting solution on the physicochemical properties of zinc ferrite synthesized at low temperature. *Journal of Alloys and Compounds*, 287(1–2), 276–283. https://doi.org/10.1016/S0925-8388(99)00069-9
- Ding, J., Liu, X., Wang, J., & Shi, Y. (2000). Ultrafine ferrite particles prepared by coprecipitation/mechanical milling. *Materials Letters*, 44(1), 19–22. https://doi.org/10.1016/S0167-577X(99)00290-6
- El-Eskandarany, M., Al-Hazza, A., Al-Hajji, L., Ali, N., Al-Duweesh, A., Banyan, M., & Al-Ajmi, F. (2021). Mechanical milling: a superior nanotechnological tool for fabrication of nanocrystalline and nanocomposite materials. *Nanomaterials*, *11*(10), 2484. https://doi.org/10.3390/nano11102484
- Fuentes, A., & Takacs, L. (2013). Preparation of multicomponent oxides by mechanochemical methods. *Journal of Materials Science*, 48(2), 598–611. https://doi.org/10.1007/s10853-012-6909-x
- Garg, J., Chiu, M., Krishnan, S., Kumar, R., Rifah, M., Ahlawat, P., & Gupta, P. (2024). Emerging trends in zinc ferrite nanoparticles for biomedical and environmental applications. *Applied Biochemistry and Biotechnology*, *196*(2), 1008–1043. https://doi.org/10.1007/s12010-023-04570-2
- García, R., Suarez, G., Pech, W., Ordonez, L., Melendez, P., Sanchez, N., & González, D. (2024). Soft chemistry synthesis of size-controlled ZnO nanostructures as photoanode for dye-sensitized solar cell. *Revista Mexicana de Ingeniería Química*, 23(2). https://doi.org/10.24275/rmiq/IE24235
- Gnanaprakash, G., Mahadevan, S., Jayakumar, T., Kalyanasundaram, P., Philip, J., & Raj, B. (2007). Effect of initial pH and temperature of iron salt solutions on formation of magnetite nanoparticles. *Materials Chemistry and Physics*, 103(1), 168–175. https://doi.org/10.1016/j.matchemphys.2007.02.011
- Hejazi, A., Al-Hunaiti, A., Bsoul, I., Mohaidat, Q., & Mahmood, S. (2024). Optimizing the synthesis of ZnFe₂O₄ through chemical and physical methods: effects of the synthesis route on the phase purity, inversion, and magnetic properties of spinel zinc ferrite. *Physica Scripta*, 99(6), 065029. https://doi.org/10.1088/1402-4896/ad4746

- James, S., Adams, C., Bolm, C., Braga, D., Collier, P., Friščić, T., & Waddell, D. (2012). Mechanochemistry: opportunities for new and cleaner synthesis. *Chemical Society Reviews*, 41(1), 413–447. https://doi.org/10.1039/C1CS15171A
- Koch, C. (1993). The synthesis and structure of nanocrystalline materials produced by mechanical attrition: A review. *Nanostructured Materials*, 2(2), 109–129. https://doi.org/10.1016/0965-9773(93)90016-5
- Leal, J., Almaral, J., Hurtado, A., Cortez, M., Bórquez, A., García, B., & Flores, J. (2024). Structural and chemical analysis of Zn ion exchange in thermally modified zeolite A4. *Revista Mexicana de Ingeniera Química*, 23(3), Mat24264. https://doi.org/10.24275/rmig/Mat24264
- Mahdikhah, V., Ataie, A., Babaei, A., Sheibani, S., Ow-Yang, C., & Abkenar, S. (2019). Control of structural and magnetic characteristics of cobalt ferrite by post-calcination mechanical milling. *Journal of Physics and Chemistry of Solids*, 134, 286–294. https://doi.org/10.1016/j.jpcs.2019.06.018
- Méndez, N., Apátiga, L., Rivera, E., Manzano, A., Gonzalez, C., & Zamora, M. (2019). Crystal growth of hydroxyapatite microplates synthesised by Sol–Gel method. *Micro & Nano Letters*, 14(14), 1414–1417. https://doi.org/10.1049/mnl.2019.0402
- Moghaddam, K., & Ataie, A. (2006). Role of intermediate milling in the processing of nanosize particles of barium hexaferrite via coprecipitation method. *Journal of Alloys and Compounds*, 426(1-2), 415-419. https://doi.org/10.1016/j.jallcom.2006.02.038
- Moravvej-Farshi, F., Amishi, M., & Nekouee, K. (2020). Influence of different milling time on synthesized Ni–Zn ferrite properties by mechanical alloying method. *Journal of Materials Science: Materials in Electronics*, *31*, 13610–13619. https://doi.org/10.1007/s10854-020-03917-3
- Navidpour, A., & Fakhrzad, M. (2020). Photocatalytic and magnetic properties of ZnFe₂O₄ nanoparticles synthesised by mechanical alloying. *International Journal of Environmental Analytical Chemistry*, 102(3), 690-706. https://doi.org/10.1080/03067319. 2020.1726331
- Pedrosa, F., Rial, J., Golasinski, K., Guzik, M., Quesada, A., Fernández, J., & Bollero, A. (2016).

- Towards high performance CoFe₂O₄ isotropic nanocrystalline powder for permanent magnet applications. *Applied Physics Letters*, *109*(22). https://doi.org/10.1063/1.4969064
- Park, J., Oh, S., & Ha, B. (2001). Characterization of iron (III) oxide nanoparticles prepared by using ammonium acetate as precipitating agent. *Korean Journal of Chemical Engineering*, 18, 215-219. https://doi.org/10.1007/BF02698462
- Prime, R. B., Bair, H. E., Vyazovkin, S., Gallagher, P. K., & Riga, A. (2009). Thermogravimetric analysis (TGA). *Thermal Analysis of Polymers:* Fundamentals and Applications, 241-317.
- Rao, B., Caltun, O., Cho, W., & Kim, C. (2007). Synthesis and characterization of mixed ferrite nanoparticles. *Journal of Magnetism and Magnetic Materials*, 310(2), 812-814. https://doi.org/10.1016/j.jmmm.2006.10.771
- Sani, R., Beitollahi, A., Maksimov, Y., & Suzdalev, I. (2007). Synthesis, phase formation study and magnetic properties of CoFe₂O₄ nanopowder prepared by mechanical milling. *Journal of Materials Science*, 42, 2126-2131. https://doi.org/10.1007/s10853-006-1235-9
- Sarkar, K., Mondal, R., Dey, S., Majumder, S., & Kumar, S. (2019). Presence of mixed magnetic phase in mechanically milled nanosized Co_{0.5}Zn_{0.5}Fe₂O₄: A study on structural, magnetic and hyperfine properties. *Journal of Magnetism and Magnetic Materials*, 487, 165303. https://doi.org/10.1016/j.jmmm.2019.165303
- Shenoy, S., Joy, P., & Anantharaman, M. (2004). Effect of mechanical milling on the structural, magnetic and dielectric properties of coprecipitated ultrafine zinc ferrite. *Journal of Magnetism and Magnetic Materials*, 269(2), 217-226. https://doi.org/10.1016/S0304-8853(03)00596-1
- Shi, Y., Ding, J., Liu, X., & Wang, J. (1999). NiFe₂O₄ ultrafine particles prepared by coprecipitation/mechanical alloying. *Journal of Magnetism and Magnetic Materials*, 205(2-3), 249-254. https://doi.org/10.1016/S0304-8853(99)00504-1
- Sukmarani, G., Kusumaningrum, R., Noviyanto, A., Fauzi, F., Habieb, A., Amal, M., & Rochman, N. (2020). Synthesis of manganese ferrite from manganese ore prepared by mechanical milling and its application as an inorganic heat-resistant pigment. *Journal of Materials Research and*

- *Technology*, 9(4), 8497-8506. https://doi.org/10.1016/j.jmrt.2020.05.122
- Takacs, L. (1998). Combustion phenomena induced by ball milling. *Materials Science Forum*, 269, 513-522. https://doi.org/10.4028/ www.scientific.net/MSF.269-272.513
- Teja, A., & Koh, P. (2009). Synthesis, properties, and applications of magnetic iron oxide nanoparticles. *Progress in Crystal Growth and Characterization of Materials*, 55(1-2), 22-45. https://doi.org/10.1016/j.pcrysgrow. 2008.08.003
- Thanh, N., Maclean, N., & Mahiddine, S. (2014). Mechanisms of nucleation and growth of nanoparticles in solution. *Chemical Reviews*, 114(15), 7610-7630. https://doi.org/10.1021/cr400544s
- Tomiczek, A. (2021). Effect of milling time on microstructure of cobalt ferrites synthesized by mechanical alloying. *Archives of Materials Science and Engineering*, 111(1). https://doi.org/10.5604/01.3001.0015.5561
- TIP, T. (2023). Interpreting DSC curves Part 1: Dynamic measurements.
- Tehranian, P., Shokuhfar, A., & Bakhshi, H. (2019). Tuning the magnetic properties of ZnFe₂O₄ nanoparticles through partial doping and annealing. *Journal of Superconductivity and Novel Magnetism*, 32, 1013-1025. https://doi.org/10.1007/s10948-018-4785-6
- Verwey, E., & Heilmann, E. (1947). Physical properties and cation arrangement of oxides with spinel structures. *Journal of Chemical Physics*, *15*, 174-180. https://doi.org/10.1063/1.1746464
- Wang, Q., Liang, E., & Wang, C. (2024). High performance bismuth titanate-ferrite piezoelectric ceramics for high-temperature applications. *Journal of the European Ceramic Society*, 44(8), 5080-5087. https://doi.org/10.1016/j.jeurceramsoc.2024.02.017
- Wyckoff, R. (1963). *Crystal Structures* (Vol. 1). Interscience Publishers.
- Younes, A., Kherrouba, N., & Bouamer, A. (2021). Magnetic, optical, structural and thermal properties of copper ferrite nanostructured synthesized by mechanical alloying. *Micro & Nano Letters*, 16(4), 251-256. https://doi.org/10.1049/mna2.12040

11

Zhang, C., Zhong, X., Yu, H., Liu, Z., & Zeng, D. C. (2009). Effects of cobalt doping on the microstructure and magnetic properties of Mn-Zn ferrites prepared by the co-precipitation method. *Physica B: Condensed Matter*, 404(16), 2327-2331. https://doi.org/10.1016/j.physb.2008.12.044

Zhang, F., Su, Z., Wen, F., & Li, F. (2008). Synthesis and characterization of polystyrene-

Synthesis and characterization of polystyre

grafted magnetite nanoparticles. *Colloid and Polymer Science*, 286, 837-841. https://doi.org/10.1007/s00396-008-1854-6

Zhang, Z., Yao, G., Zhang, X., Ma, J., & Lin, H. (2015). Synthesis and characterization of nickel ferrite nanoparticles via planetary ball milling assisted solid-state reaction. *Ceramics International*, 41(3), 4523-4530. https://doi.org/10.1016/j.ceramint.2014.11.147

Appendix

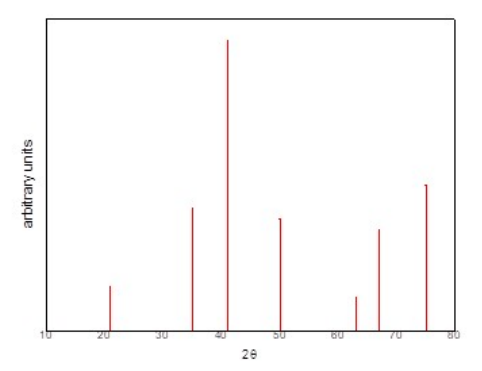


Fig. A.1. X-ray diffraction pattern of magnetite according to Aliramaji *et al.* (2015).

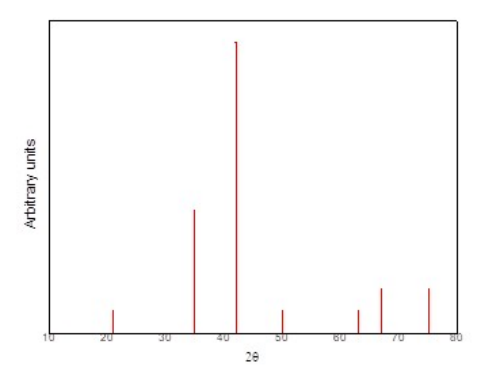


Fig. A.2. X-ray diffraction pattern of $ZnFe_2O_4$ according to Tehranian *et al.* (2019).